

GT2004-53863

**EVALUATING THE STABILITY OF BSAS-BASED EBCs
IN HIGH WATER-VAPOR PRESSURE ENVIRONMENTS**

Karren L. More and Peter F. Tortorelli

Oak Ridge National Laboratory, Oak Ridge, Tennessee

Tania Bhatia and G.D. Linsey

United Technologies Research Center, East Hartford, Connecticut

ABSTRACT

Barium Strontium Aluminosilicate (BSAS)-based environmental barrier coatings (EBCs) have been used successfully to protect the surface of Si-based fiber-reinforced ceramic-matrix composite (CMC) combustor liners in Solar Turbines Centaur 50S gas turbine engines. Two such EBC/CMC combustor liner sets were engine-exposed for times >14,000h. However, extensive microstructural characterization of the EBC/CMC liners after the long-term engine exposures showed a significant loss/recession of the BSAS-based EBC. The mechanisms by which BSAS recession occurs and the rate at which the BSAS recesses as a function of pressure, gas velocity, temperature, etc. are not fully understood but such information will be necessary for improving the life to >>15,000h in order for the materials to be acceptable for use in an engine application. To this end, the thermochemical stabilities of candidate EBCs are being evaluated analytically and experimentally at very high H₂O pressures in a high-temperature, high-pressure furnace (Oak Ridge National Laboratory's "Keiser Rig"). Calculations based on generalized volatility reactions and mass flux of volatilized species have shown that high H₂O pressures can be used to compensate for the low gas-flow velocities in the Keiser Rig. An examination of the phase stability/volatilization of state-of-the-art EBC compositions (Ba- and Sr-based aluminosilicates) has been conducted through equilibrium thermodynamic calculations and initial experiments to validate assumptions via Keiser Rig exposures of the same EBC formulations conducted at 1250°C and 20 atm H₂O.

INTRODUCTION

Structural, Si-based ceramic materials (SiC, SiC/SiC CMCs, Si₃N₄) are being developed for use as hot section components in gas turbine and microturbine engines as a result of their excellent high-temperature stability and property retention when compared with their metallic counterparts. However, the exposure of unprotected Si-based materials to the high temperature and high water-vapor pressures typical of gas turbine combustion environments results in rapid

oxidation [1-6] and surface loss/recession due to SiO₂ volatilization.[7,8] There has been a significant amount of research during the past several years in the area of EBC development for the protection of Si-based CMCs and monolithics.[9,10] Protective surface coatings (specifically EBCs) are absolutely required to prevent degradation of oxidation- and volatilization-susceptible ceramic substrates during use in high H₂O pressure environments typical of combustion turbines.

Environmental barrier coatings based on the BSAS and mullite system are the current system of choice for engine hot-section components.[11-13] These EBCs were initially developed as part of NASA's High Speed Civil Transport and Enabling Propulsion Materials Programs. The same EBC system was optimized and scaled-up under the U.S. Department of Energy's Ceramic Stationary Gas Turbine Program for application on SiC/SiC CMC combustor liners utilized in a Solar Turbines Centaur 50S gas turbine. As part of the CSGT Program, CMC/EBC liners ran in the two most recently-completed engine tests for 13,937 h [11,12] and 15,144 h.[13] The application of EBCs to the gas-path surfaces significantly increased the combustor liner engine-life compared with unprotected SiC/SiC liners, however, several life-limiting factors were identified following the long-term engine tests, the most significant of which was volatilization of the BSAS top coat.[11-13]

The measurable volatilization of the BSAS phase during engine testing was unexpected and demonstrated the critical need for an inexpensive laboratory exposure test to screen candidate EBC compositions for volatility before testing in an actual engine. The high-temperature, high-pressure exposure facility at Oak Ridge National Laboratory (ORNL) has been used to screen EBCs at relatively high H₂O pressures (0.3-2.0 atm) in terms of (1) thermal stability of the coating and interfacial region at elevated temperature (1100°C-1350°C) and (2) permeation resistance to oxidizing species (primarily steam). [14] Because of the low gas-flow velocities in the Keiser Rig (5-33X10⁻⁴ m/s), volatilization could not be fully assessed. More recently, as a result of the BSAS volatilization observed during

the two long-term engine tests, the potential use of the Keiser Rig to evaluate volatility of candidate EBCs has been explored. Calculations based on generalized volatility reactions and mass flux of volatilized species have shown that high H₂O pressures can be used to compensate for the low gas-flow velocities used in the Keiser Rig. Substantial fluxes of volatile species can be obtained by increasing the H₂O pressure from 1.5 atm (typical value corresponding to water vapor-pressure in a gas turbine combustor) to 20 atm. High H₂O pressure exposures are currently being conducted in a modified Keiser Rig to validate the analytical treatments (described in detail below). Initial results from these experiments are presented.

EXPERIMENTAL PROCEDURE

All laboratory exposures were conducted in ORNL's high-temperature, high-pressure facility which comprises three different "Keiser Rigs". The Keiser Rig used for this study consisted of a large box furnace which contained two 92 cm long X 9 cm diameter SiC pressure vessels and a multiple-flow gas-supply/manifold system, as shown in Figure 1.[15] Samples are hung on the outside of a slotted alumina tube using Pt wire which is suspended inside a SiC tube.[6] A slow-flow gas supply system ($5\text{-}33 \times 10^{-4}$ m/s) provides a pressurized mixture of steam and air to each SiC tube. Previous high-temperature, high-pressure exposures of EBC/CMC materials in the Keiser Rig were conducted to evaluate the thermal-stability and protective-capability of different EBC formulations using exposure conditions which best simulated the temperature, pressure, and principal reactive gas species (H₂O) of combustor environments.[6,14] For example, to evaluate materials for use in a Solar Turbines Centaur 50S engine, all Keiser Rig exposures of EBC/SiC-SiC CMCs were conducted at ~1200°C (2200°F), 1.5 atm H₂O (balance air), and 10 atm total system pressure. In the present study, an extremely high H₂O pressure (20 atm) and elevated temperature (1250°C) are being utilized to:

- (1) validate that very high water vapor-pressures can be used to induce volatility in the Keiser Rig (i.e., high H₂O pressures to compensate for low gas-flow velocities in the Keiser Rig)
- (2) to measure the volatility of candidate EBCs.

To accommodate the much higher water-vapor pressures used in this study (compared to conditions typically used in previous exposures), several modifications were made to the Keiser Rig's gas supply and exhaust systems (described in detail in subsequent section).

There were several "proof-of-principle" specimens included in the initial high water-vapor-pressure exposures to demonstrate and measure volatilization in the Keiser Rig. High purity SiC (produced by chemical vapor deposition) and quartz have been well-characterized after exposure to high water vapor-pressures [1,16] and were included as standards in the initial high-pressure Keiser Rig runs. Also, since the primary purpose of these experiments was to measure the volatilization rates of currently-used, state-of-the-art EBCs, specimens of plasma-sprayed BSAS (mechanically removed from the surface of an EBC/CMC) as well hot-pressed BSAS, Barium Aluminosilicate (BAS), and Strontium Aluminosilicate (SAS) materials were exposed simultaneously with the standards. The hot-pressed oxides were prepared by United Technologies Research Center. The 7.5 cm X 7.5 cm hot-pressed plates were each cut into six 2.5 cm X 2.5 cm coupons. All of the samples to be exposed in the ORNL furnace had their surfaces mechanically ground flat and parallel and polished with 6 μm diamond paste. Each sample was weighed and measured. The BSAS, BAS, and SAS coupons were also microstructurally characterized in the as-processed condition for comparison with the same material after

exposure in the Keiser Rig. Pre- and post-exposure cross-section specimens were imaged in a scanning electron microscope (SEM) equipped with a backscatter detector and compositionally analyzed using an electron probe microanalyzer (EPMA). In this way, reaction products (or lack thereof) that formed during exposure, as well as any other microstructural changes, were identified, characterized with respect to their spatial dimensions, and compared to the as-processed microstructures.

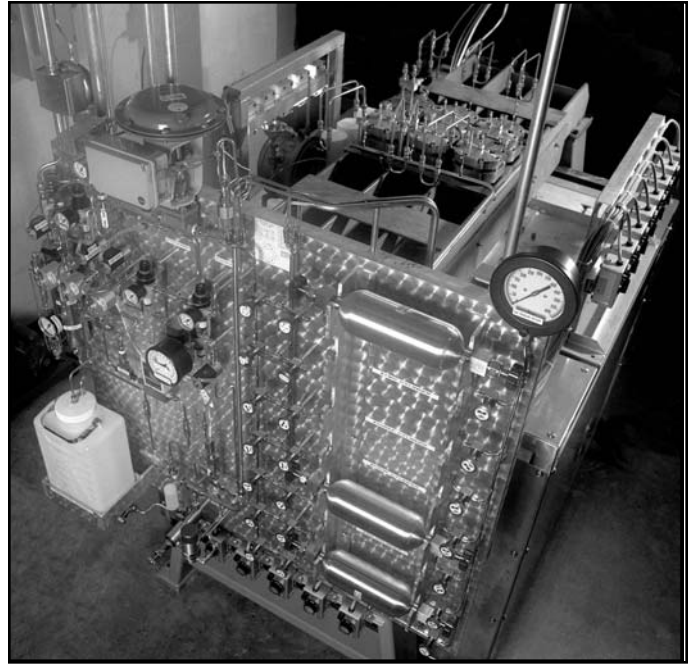


Fig. 1. The ORNL Keiser Rig used in the current experiments consisted of a large box furnace and gas supply systems for 2 SiC tubes.

EVALUATING VOLATILITY AT HIGH H₂O PRESSURES IN ORNL'S KEISER RIG

Volatilization of Si-based ceramics can be the life-limiting factor for the use of these materials in combustion environments, where high temperatures, elevated oxidizing potentials, and significant gas-flow velocities exacerbate the volatilization process. This degradation mechanism has been shown to be of specific relevance for SiC and Si₃N₄, where SiO₂ forms by oxidation and then readily reacts with environmental H₂O to form volatile species.[7,8,17,18] Of the various volatilization reactions, the one forming Si(OH)₄,



has been shown to be predominant in combustion environments.[18] It is therefore of interest to examine the various factors involved in volatilization under oxidizing conditions as part of studies that are aimed at developing and characterizing materials that are stable at the high water-vapor pressures associated with various combustion conditions.

For the present work, it is assumed that the release of a volatile species is controlled by diffusion through a gaseous boundary layer adjacent to the solid oxide surface under laminar-flow conditions.

These assumptions have been shown to be appropriate for combustion associated with moderate gas-flow velocities (~40 m/s) [18] and should also apply to the slow-flow, large-diameter, flat-specimen conditions of the Keiser Rig. The mass flux associated with volatilization, \mathbf{J} , can be described as [18]

$$\mathbf{J} \propto (\rho'vL/\eta)^{1/2}(\eta/\rho'D)^{1/3}(Dp/L) \quad (2)$$

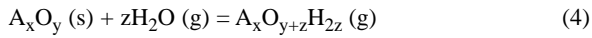
where v is the linear gas velocity, η is the gas viscosity, D is the interdiffusion coefficient of the volatile species in the major gas component, ρ is the concentration of the volatile species at the solid-gas interface, ρ' is the concentration of the major gas component, and L is the characteristic specimen length parallel to the flow direction and over which the volatility is averaged.

For the conditions associated with the Keiser Rig, equation (2) reduces to

$$\mathbf{J} \propto (v^{1/2} \cdot \Sigma p_{vol}) / (p_{tot})^{1/2} \quad (3)$$

where p_{vol} is the partial pressure of a volatile species and p_{tot} is the total system pressure.

For the present case, in which the primary interest is in volatilization of oxides in the presence of water vapor, the formation of a volatile hydroxide product, $A_xO_{y+z}H_{2z}$, can be generally represented as



The equilibrium constant for this reaction, K_4 , can be expressed in terms of the activity of the oxide, $a_{A_xO_y}$, and partial pressures as

$$K_4 = p_{A_xO_{y+z}H_{2z}} / (p_{H_2O}^z \cdot a_{A_xO_y}) \quad (5)$$

and is also related to the free energy of formation of $A_xO_{y+z}H_{2z}$, $G_{A_xO_{y+z}H_{2z}}$:

$$K_4 = \exp(-G_{A_xO_{y+z}H_{2z}}/RT) \quad (6)$$

where T is the absolute temperature and R is the universal gas constant. Combining equations (5) and (6) yields

$$p_{A_xO_{y+z}H_{2z}} = \exp(-G_{A_xO_{y+z}H_{2z}}/RT) \cdot p_{H_2O}^z \cdot a_{A_xO_y} \quad (7)$$

Assuming the reaction shown in equation (4) generates the only volatile species and using equation (3), the mass flux of volatile species can be described as

$$\mathbf{J} \propto v^{1/2} \cdot \exp(-G_{A_xO_{y+z}H_{2z}}/RT) \cdot p_{H_2O}^z \cdot a_{A_xO_y} / (p_{tot})^{1/2} \quad (8)$$

A flux equation of the form shown in equation (8) has been shown to describe measurements of SiC and Si₃N₄ recession controlled by volatilization of SiO₂ quite well.[8,17] However, at low gas-flow velocities and modest pressures, as employed in many laboratory experiments, specimen mass losses due to volatilization are small (equation (8)) and, thus, difficult to measure, particularly because of large mass gains due to accelerated solid-state oxidation at elevated p_{H₂O}. [1,2,16] This was the case for experiments previously conducted in the Keiser Rig, which focused on the effects of elevated H₂O

pressures (typically 0.3-2.0 atm) on oxidation of Si-based ceramics and environmental barrier coatings.[2,6,14,16] However, as shown by equation (8), mass fluxes for a given v can be increased substantially by using higher H₂O pressures, particularly if $z > 1$.

An example of how higher H₂O pressures can be used to generate more readily measurable mass fluxes can be determined from that of SiO₂ (equation (1)), where, from equations (4) and (8)

$$\mathbf{J} \propto v^{1/2} \cdot \exp(-G_{Si(OH)_4}/RT) \cdot p_{H_2O}^2 \cdot a_{SiO_2} / (p_{tot})^{1/2} \quad (9)$$

and $a_{SiO_2} = 1$. Relatively high fluxes of Si(OH)₄ can be achieved by increasing p_{H₂O} since \mathbf{J} is proportional to the square of the water-vapor pressure. Therefore, if there is no change in mechanism, low gas-flow velocities can be offset by higher p_{H₂O}. This is illustrated in Figure 2, which plots \mathbf{J}/\mathbf{J}_0 versus p_{H₂O} for the case represented by equation (9) where \mathbf{J}_0 is the Si(OH)₄ flux for typical combustor liner conditions ($v=35$ m/s, p_{H₂O}=1.5 atm, T=1200°C) and \mathbf{J} is for the same temperature with $v = 6 \times 10^{-4}$ m/s (typical gas-flow velocity in the Keiser Rig). Note from Figure 2 that the normalized flux can be increased by approximately two orders of magnitude by increasing p_{H₂O} from 1.5 atm (pressure typically used) to 20 atm.

The results shown in Figure 2 show that the high-temperature, high-pressure capability offered by a Keiser Rig (or similar exposure facility) can be used to yield relatively high volatility fluxes by conducting experiments at substantially higher water-vapor pressures. As such, this approach can be used to screen the volatility resistance of candidate ceramics for use in combustion environments as bulk materials or protective surface coatings (such as needed for EBCs). However, such use is predicated on no change in the rate-controlling volatilization mechanism as the water-vapor pressure is increased. Given the nature of the process described above (diffusion of volatile product across a laminar gas-boundary region), it is not expected that changes in pressures over the range indicated in Figure 2

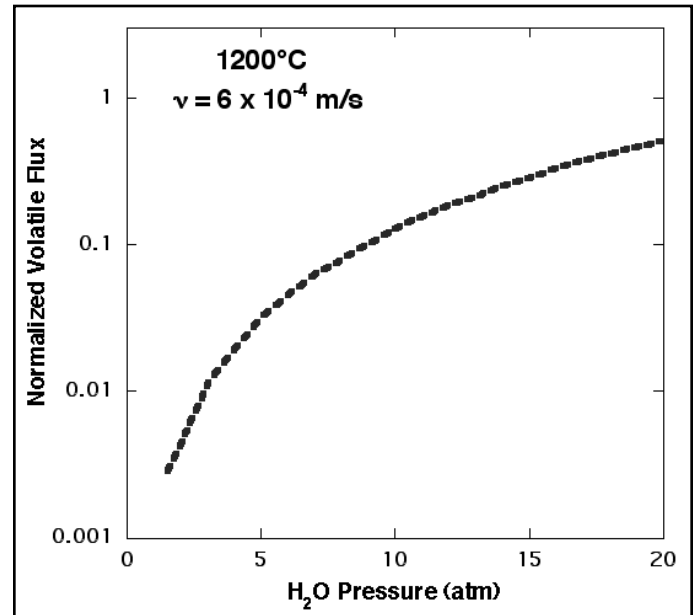


Figure 2. Plot of flux of Si(OH)₄ due to volatilization of SiO₂ in an H₂O-containing environment at 1200°C, a total pressure of 20 atm, and a gas flow velocity of 6X10⁻⁴ m/s as a function of the partial pressure of H₂O.

would result in a change in mechanism.

Referring to equation (8), it is important to note that the ability to use higher water-vapor pressures to screen the volatilization resistance of candidate materials in systems using low gas-flow velocities depends critically on z , the number of moles of H_2O needed to form one mole of volatile product (see equation (4)). A low z value would make it more difficult to achieve easily measurable volatile fluxes by increasing the water-vapor pressure over a reasonable range. As an example, the difference in the normalized flux between $z=1$ and $z=2$ is shown in Figure 3 for $v=6 \times 10^{-4}$ m/s and $1200^\circ C$. While there is about an order of magnitude increase in the volatile flux when p_{H_2O} is increased from 1.5 to 20 atm for $z=1$, this enhancement is still about 10X less than for $z=2$. Thus, it is important to understand the nature of the predominant volatility reaction (equation (4)) to determine if p_{H_2O} elevation will yield the desired measurements and to effectively compare relative results for J for different oxides.

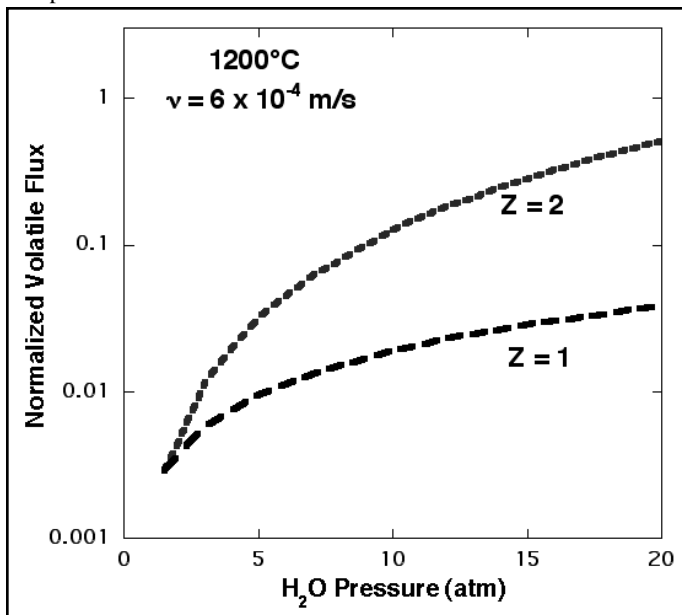


Figure 3. Plot of flux of a volatile species in an H_2O -containing environment at $1200^\circ C$, a total pressure of 20 atm, and a gas flow velocity of 6×10^{-4} m/s as a function of z and of the partial pressure of H_2O .

Besides z , there are other factors that need to be considered in analyzing volatility results from such experiments. As shown in equation (3), the total volatile flux is a sum of all potential reactions, so it is possible to have measured values that are not specific to one species if there are several products with comparable vapor pressures. This can be the case for complex mixed oxides with different z values and/or that form oxides as well as hydroxides with high vapor pressures. Strict interpretation of results from such mixed oxides will also be complicated by uncertainties in the activities of the various components (see equation (8)) as these may deviate significantly from what is expected for ideal solution behavior.

INITIAL MATERIAL EXPOSURES AT HIGH H_2O PRESSURES

The initial Keiser Rig exposure at 20 atm (~18 atm H_2O) and $1250^\circ C$ ended prematurely (after < 100 h at temperature and pressure)

when the SiC pressure vessel failed. All the samples included in this run were destroyed. It was assumed that the SiC tube had a critical flaw unable to withstand the higher pressures utilized in the experiment.

The second Keiser Rig exposure at 18.2 atm H_2O (20 atm total pressure) and $1250^\circ C$ also ended prematurely due to another SiC tube failure, but in this case, ~328 h of sample exposure had accumulated. Subsequent examination of the day-to-day furnace/rig operation data accumulated during the run revealed that the use of the very high H_2O pressures had caused problems apparently related to volatilization of products from the SiC containment tube and specimens. The outlet (exhaust) lines and filters for the flowing H_2O -laden gas and the backpressure regulating valve accumulated deposits of volatile species which led to malfunction of the valve and consequent failure of the SiC tube by overpressurization. In addition to a premature end of the exposure period (originally scheduled for 500 h) and loss of many specimens, failure also caused extensive damage to the furnace's insulation and heating elements, which had to be replaced. To avoid future problems, the gas supply and exhaust systems were modified; filters with higher-conductance manifolding were installed to protect the regulating valve and all the 0.3175 and 0.635 cm (OD) gas lines were replaced with 0.9525 cm tubing to prevent plugging by deposits (between regularly scheduled maintenance periods). The outlet system has been redesigned so that filters can be easily replaced after each run (typically 500 h). A pressure relief valve was installed on the gas inlet side.

Following the second high-pressure run in the Keiser Rig, the BSAS, BAS, and SAS samples were salvaged from the bottom of the furnace (albeit with somewhat damaged surface areas) after being exposed for 328 h. The standard samples (CVD SiC and quartz) were not recovered. Since the three oxide samples salvaged after the explosion were only slightly damaged, an analysis was conducted to determine whether any volatilization had occurred during the run at 18.2 atm H_2O .

The as-processed microstructures of the three oxide samples are shown in Figures 4, 5, and 6, for the hot-pressed BAS, SAS, and BSAS, respectively. Each of the oxides exhibited a 2-phase structure (brightly-imaging dispersed second phase) and extensive porosity in the as-fabricated state. The matrix composition for each oxide is given in Table I along with the composition of the second phase (as determined by EPMA). X-ray diffraction data identifying the major crystalline phase in each specimen are also given in Table I.

After exposure for 328 h at $1250^\circ C$ and 18.2 atm H_2O , the thickness of each sample was measured from undamaged specimen areas (mass measurements were not reliable due to tube failure). For the BAS and BSAS specimens, an ~8% increase in specimen thickness occurred while the SAS specimen exhibited an ~2% thickness decrease. Microstructural changes for each oxide specimen were also characterized after exposure. X-ray diffraction data from exposed surfaces of the SAS and BSAS samples showed no change in the major crystalline phase due to high-temperature, high- H_2O -pressure exposure. The data for BAS showed only $BaAl_2Si_2O_8$ with no unidentified second phase (as observed in as-fabricated BAS, Table 1). Comparable BSE images (to Figures 4, 5, and 6) for the BAS, SAS, and BSAS cross-sections after exposure for 328 h are shown in Figures 7, 8, and 9, respectively.

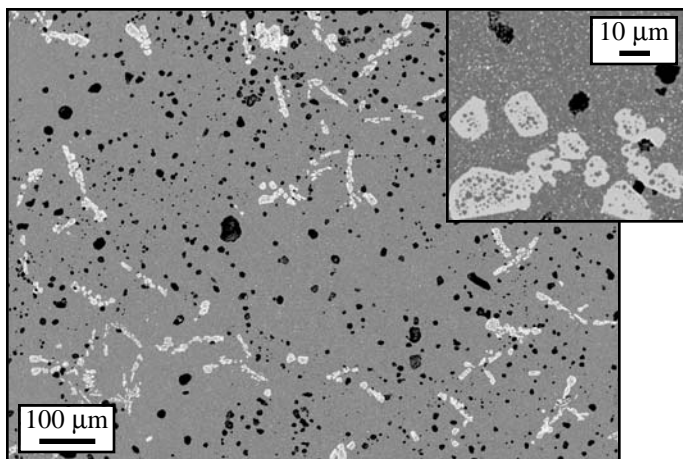


Figure 4. As-processed microstructure of hot-pressed BAS. Inset micrograph shows distribution of second phase particles.

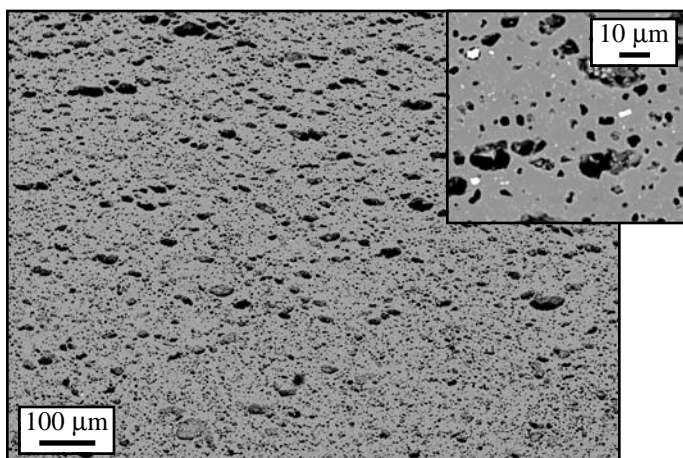


Figure 5. As-processed microstructure of hot-pressed SAS. Inset micrograph shows distribution of second phase particles.

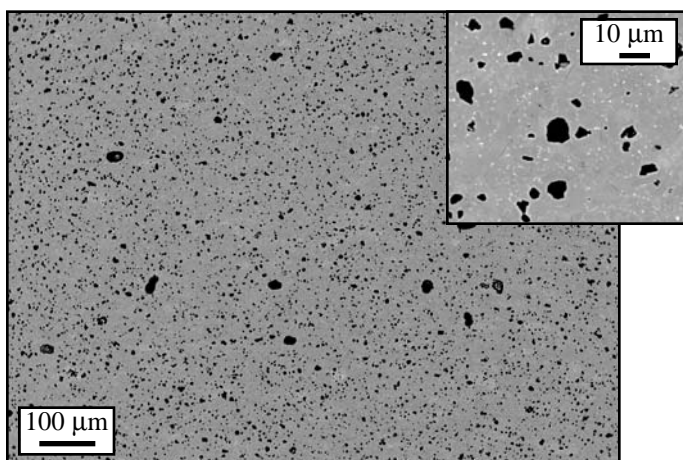


Figure 6. As-processed microstructure of hot-pressed BSAS. Inset micrograph shows distribution of second phase particles.

	BAS	SAS	BSAS
Matrix Phase Composition (at%)	Ba 7.9 Al 15.5 Si 15.0 O 61.6	Sr 7.6 Al 15.1 Si 15.6 O 61.7	Ba 5.9 Sr 1.8 Al 15.4 Si 15.3 O 61.6
Secondary Phase Composition (at%)	Ba 10.8 Al 18.4 Si 10.5 O 60.3	Sr 8.8 Al 13.0 Si 16.0 O 62.2	Ba 5.4 Sr 4.3 Al 14.4 Si 13.7 O 62.2
Primary Crystalline Phase (XRD)	$\text{BaAl}_2\text{Si}_2\text{O}_8$ <small>(major second phase not identified by XRD)</small>	$\text{SrAl}_2\text{Si}_2\text{O}_8$	$\text{Ba}_{0.75}\text{Sr}_{0.25}\text{Al}_2\text{Si}_2\text{O}_8$

Table 1. Composition and X-ray diffraction data for as-processed BAS, SAS, and BSAS materials used for Keiser Rig exposures.

Microstructural analysis was conducted not only to evaluate bulk microstructural changes in the specimens as a result of exposure to the high H_2O pressures, but to assess any material recession/loss or change in surface structure/composition after exposure. As evidenced in Figures 7, 8, and 9, surface morphological changes were observed for all three oxide specimens after exposure. Clear densification of the surfaces accompanied by changes in phase distribution were noted for each sample and was especially evident for the BAS. Figure 7(a) shows that the BAS underwent extensive grain growth (recrystallization) and redistribution of the porosity and second phase at the surface. A denser surface region $\sim 400 \mu\text{m}$ thick was completely devoid of the Ba-rich second phase (identified in the as-fabricated BAS) and was composed of an intimate 2-phase mixture of the $\text{BaAl}_2\text{Si}_2\text{O}_8$ matrix phase and a more predominant Si-rich (23 at%), Al-poor (6.1 at%), isostructural phase (shown clearly in Figure 7(b)). Phase separation (into SiO_2 -rich phase(s)) will likely precede any volatilization reactions since recession of the BAS (as well as BSAS and SAS) will occur due to preferential volatilization of silica from the oxide.[19] The BAS specimen has undergone the initial stage of phase separation with minimal (if any) volatilization after only 328 h exposure. The 8% thickness increase measured after exposure is most likely due to significant BAS grain growth and an increase in porosity.

The SAS specimen also exhibited a very dense surface region $\sim 75 \mu\text{m}$ thick post-exposure at 18.2 atm for 328 h. However, the extensive bulk grain growth and porosity redistribution observed in the BAS was not observed for SAS. The SAS dense surface region (Figure 8(a)) was, for the most part, void of any Sr-rich second phase and also showed the start of phase separation (similar to that observed for the BAS, but on a much finer scale) consisting of the $\text{SrAl}_2\text{Si}_2\text{O}_8$ matrix phase dispersed throughout an isostructural phase which was Si-rich (18.9 at%) and Al-poor (11.5 at%). The distribution of the two surface phases is shown in Figure 8(b). The SAS specimen was the only specimen to show a thickness decrease (2%) after exposure which was likely due to shrinkage associated with the observed surface densification.

The surface of the BSAS specimen is shown in Figure 9(a). The BSAS surface (50-80 μm) was densified to some extent during exposure to high H_2O pressures for 328 h, but grain growth and pore size changes were not evident. The top 10-20 μm of the BSAS surface showed the highest density (see Figure 9(b)) and this dense region was single phase $\text{Ba}_{0.5}\text{Sr}_{0.5}\text{Al}_2\text{Si}_2\text{O}_8$ rather than the $\text{Ba}_{0.75}\text{Sr}_{0.25}\text{Al}_2\text{Si}_2\text{O}_8$ celsian phase identified in the as-processed BSAS. Below this dense outermost surface layer, a small amount of phase-separation to BSAS phase and a Si-rich (16.5 at%), Al-poor (14.3 at%) phase was observed. It is yet unclear why a significant thickness increase ($\sim 8\%$) was measured on this specimen after exposure.

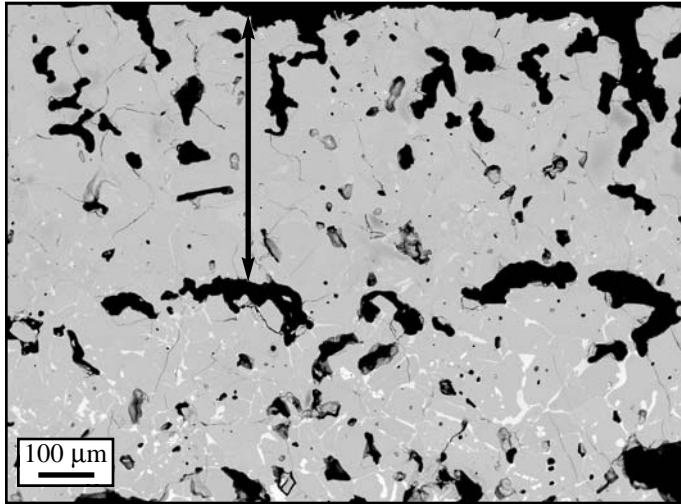


Figure 7(a). Surface of BAS after exposure in Keiser Rig for 328 h at 1250°C and 18.2 atm H_2O . Densified surface region (shown by arrows) is void of Ba-rich second phase.

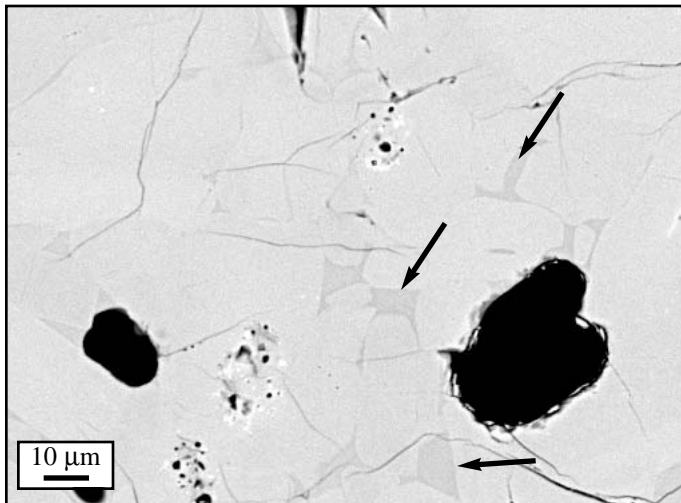


Figure 7(b). Within densified surface of BAS after exposure in Keiser Rig for 328 h at 1250°C and 18.2 atm H_2O . A 2-phase structure is apparent in the densified surface region consisting of (minor) $\text{BaAl}_2\text{Si}_2\text{O}_8$ (shown by arrows) and a (major) Si-rich (23 at%), Al-poor (6.1 at%) phase.

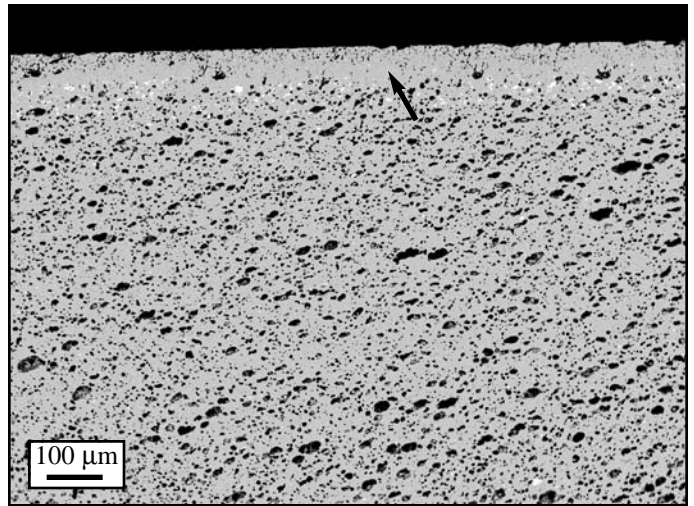


Figure 8(a). Surface of SAS after exposure in Keiser Rig for 328 h at 1250°C and 18.2 atm H_2O . Densified surface region (shown by arrows) is void of Sr-rich second phase.

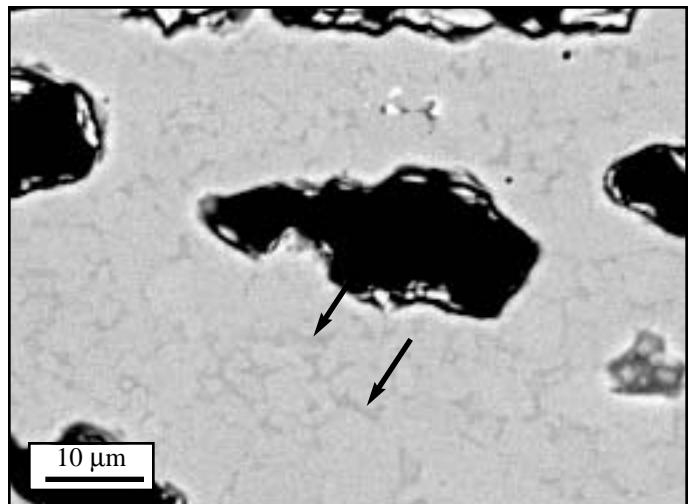


Figure 8(b). Within densified surface of SAS after exposure in Keiser Rig for 328 h at 1250°C and 18.2 atm H_2O . A 2-phase structure is apparent in the densified surface region consisting of the (minor) $\text{SrAl}_2\text{Si}_2\text{O}_8$ matrix (shown by arrows) and an isostructural (major) phase which was Si-rich (18.9 at%) and Al-poor (11.5 at%).

CONCLUSIONS

A high-temperature, high-pressure furnace (ORNL's Keiser Rig) has been modified to accommodate very high H_2O pressures of 20 atm. Keiser Rig exposures have previously been used to accurately assess an EBC's ability to effectively protect Si-based ceramics. In the work described herein, an analysis based on volatility reactions and mass flux of volatilized species has shown that operating at very high H_2O pressures can be used to compensate for the low gas velocities ($\sim 6 \times 10^{-4}$ m/s) in the Keiser Rig. By operating at much higher H_2O pressures, the use of the Keiser Rig can be expanded to evaluate the volatility of candidate EBCs in addition to addressing EBC thermal stability and protective capability issues. An initial exposure of Ba- and Sr-based EBCs at a H_2O pressure of 18.2 atm and 1250°C for 328 h did not

necessarily validate the principles discussed in this paper, but did induce the microstructural and compositional changes that likely occur prior to the onset of volatilization (i.e., the formation of a Si-rich phase at the surface of specimens of BAS, SAS, and BSAS). Clearly, much longer exposure times will be required to evaluate the capability of using high H₂O pressures in the Keiser Rig to induce volatilization in Ba- and Sr-based EBCs. Also, successful exposures of “standard” volatilization-susceptible materials (Si, SiC, quartz) will be required.

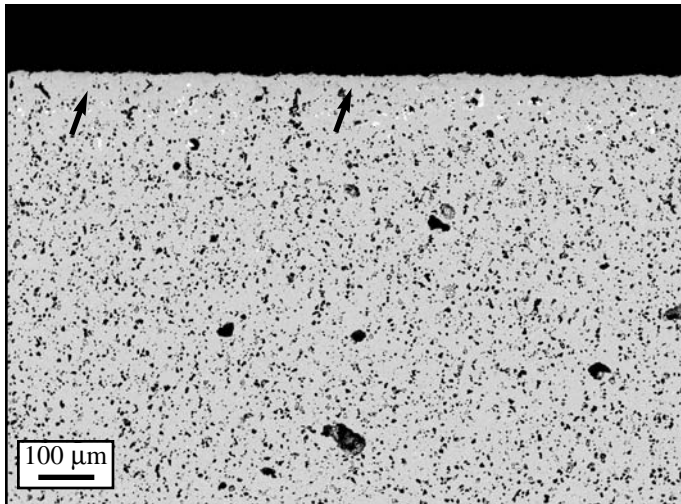


Figure 9(a). Surface of BSAS after exposure in Keiser Rig for 328 h at 1250°C and 18.2 atm H₂O. Densified surface region (shown by arrows) is void of Sr-rich second phase.

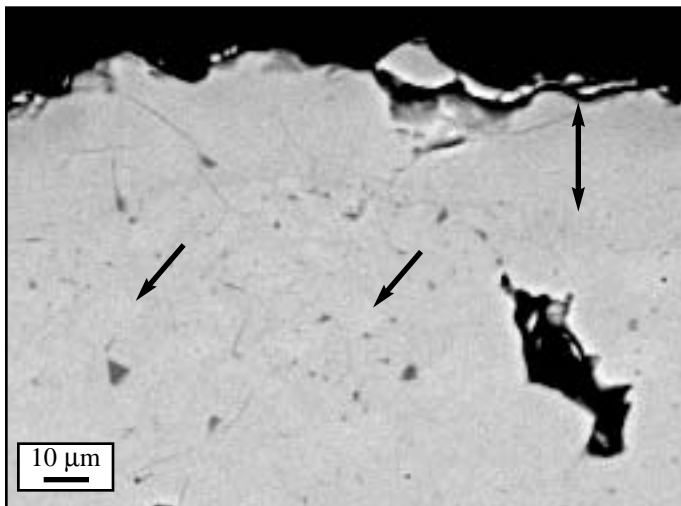


Figure 9(b). Densified Ba_{0.5}Sr_{0.5}Al₂Si₂O₈ surface of BSAS specimen after exposure in Keiser Rig for 328 h at 1250°C and 18.2 atm H₂O. A 2-phase structure is apparent below the densified surface consisting of (major) Ba_{0.75}Sr_{0.75}Al₂Si₂O₈ and a (minor) Si-rich (16.5 at%), Al-poor (14.5 at%) phase (shown by arrows).

ACKNOWLEDGEMENTS

Research sponsored by the U.S. Dept. of Energy, Office of Power Technologies, Distributed Energy Program, under Contract DE-AC05-00OR22725 with UT-Battelle, LLC. Appreciation is extended to M. Howell and J.R. Keiser for operation/modification of Keiser Rig and to T. Brummett and T.S. Geer for specimen preparation. Research at

UTRC sponsored by the Office of Naval Research (ONR) and the U.S. Department of Energy, Office of Power Technologies, Distributed Energy Program.

REFERENCES

1. More, K.L., Tortorelli, P.F., Ferber, M.K., and Keiser, J.R., 2000, “Observations of Accelerated SiC Recession by Oxidation at High Water-Vapor Pressures,” *Journal of The American Ceramic Society*, **83**[1], pp. 211-13.
2. More, K.L., Tortorelli, P.F., and Walker, L.R., Miriyala, N., Price, J.R., van Roode, M., 2003, “High-Temperature Stability of SiC-Based Composites in High-Water-Vapor-Pressure Environments,” *Journal of the American Ceramic Society*, **86**[8], pp. 1272-81.
3. Miriyala, N., Simpson, J.F., Parthasarathy, V.J., Brentnall, W.D., 1999, “The Evaluation of CFCC Liners After Field-Engine Testing in a Gas Turbine,” ASME Paper 99-GT-392.
4. Miriyala, N. and Price, J.R., 2000, “The Evaluation of CFCC Liners After Field Testing in a Gas Turbine - II,” ASME Paper 2000-GT-648.
5. Miriyala, N., Fahme, A., van Roode, M., 2001, “Ceramic Stationary Gas Turbine Program - Combustor Liner Development Summary,” ASME Paper 2001-GT-512.
6. More, K.L., Tortorelli, P.F., Ferber, M.K., Keiser, J.R., Miriyala, N., Brentnall, W.D., and Price, J.R., 2000, “Exposure of Ceramics and Ceramic Matrix Composites in Simulated and Actual Combustor Environments,” *Journal of Engineering for Gas Turbines and Power*, **122**, pp. 212-18.
7. Opila, E.J. and Hann, R.E., 1997, “Paralinear Oxidation of CVD SiC in Water Vapor,” *Journal of The American Ceramic Society*, **80**[1], pp. 197-205.
8. Robinson, R.C. and Smialek, J.L., 1999, “SiC Recession Caused by SiO₂ Scale Volatility Under Combustion Conditions: I, Experimental Results and Empirical Model,” *Journal of The American Ceramic Society*, **82**[7], pp. 1817-25.
9. Eaton, H.E., Linsey, G.D., More, K.L., Kimmel, J.B., Price, J.R., and Miriyala, N., 2000, “EBC Protection of SiC/SiC Composites in a Gas Turbine,” ASME Paper 2000-GT-631.
10. Lee, K.N., 2000, “Current Status of EBCs for Si-Based Ceramics,” *Surface Coatings and Technology*, **133-134**, pp. 1-7.
11. More, K.L., Tortorelli, P.F., Walker, L.R., Kimmel, J.B., Miriyala, N., Price, J.R., Eaton, H.E., Sun, E.Y., and Linsey, G.D., 2002, “Evaluating EBCs on Ceramic Matrix Composites After Engine and Laboratory Exposures,” ASME Paper GT-2002-30630.
12. Miriyala, N., Kimmel, J.B., Price, J.R., More, K.L., Tortorelli, P.F., Eaton, H.E., Linsey, G.D., and Sun, E.Y., 2002, “The Evaluation of CFCC Liners After Field Testing in a Gas Turbine - III,” ASME Paper GT-2002-30585.
13. Kimmel, J.B., Price, J.R., More, K.L., Tortorelli, P.F., Sun, E.Y., and Linsey, G.D., 2003, “The Evaluation of CFCC Liners After Field Testing in a Gas Turbine - IV,” ASME Paper GT-2003-38920.
14. More, K.L., Tortorelli, P.F., and Walker, L.R., 2003, “Verification and EBC’s Protective Capability by First Stage Evaluation in a High-Temperature, High-Pressure Furnace,” ASME Paper GT-2003-38923.
15. Keiser, J.R., Howell, M., Williams, J.J., and Rosenberg, R.A., 1996, “Compatibility of Selected Ceramics with Steam Reformer Environments,” *Proceedings of Corrosion/96, NACE International, Houston, TX*, Paper 140.

16. Tortorelli, P.F. and More, K.L., 2003, "Effects of High Water-Vapor Pressure on Oxidation of Silicon Carbide at 1200°C," *Journal of the American Ceramic Society*, **86**[8], pp. 1249-55.
17. Smialek, J.L., Robinson, R.C., Opila, E.J., Fox, D.S., and Jacobsen, N.S., 1999, "SiC and Si₃N₄ Scale Volatility Under Combustion Conditions," *Advanced Composite Materials*, **8**[1], pp. 33-45.
18. Opila, E.J., Smialek, J.L., Robinson, R.C., Fox, D.S., and Jacobsen, N.S., 1999, "SiC Recession Caused by SiO₂ Scale Volatility Under Combustion Conditions," *Journal of the American Ceramic Society*, **82**[7], pp. 1826-34.
19. Lee, K.N., Fox, D.S., Eldridge, J.I., Zhu, D. Robinson, R.C., Bansal, N.P., and Miller, R.A., 2003, "Upper Temperature Limit of EBCs Based on Mullite and BSAS," *Journal of the American Ceramic Society*, **86**[8], pp. 1299-1306.